Plant Soil (2023) 489:107–124
https://doi.org/10.1007/s11104-023-06001-x

RESEARCH ARTICLE

A survey of leaf phosphorus fractions and leaf economic traits among 12 co-occurring woody species on phosphorus-impoverished soils

Yuki Tsujii · Baoli Fan · Brian J. Atwell · Hans Lambers · Zhangying Lei · Ian J. Wright

Received: 30 October 2022 / Accepted: 20 March 2023 / Published online: 4 April 2023

Abstract

Background and Aims The leaf economic spectrum (LES) is related to dry mass and nutrient investments towards photosynthetic processes and leaf structures, and to the duration of returns on those investments (leaf lifespan, LL). Phosphorus (P) is a key limiting nutrient for plant growth, yet it is unclear how the allocation of leaf P among different functions is coordinated with the LES. We addressed this question among 12 evergreen woody species co-occurring on P-impoverished soils in south-eastern Australia.

Methods Leaf 'economic' traits, including LL, leaf mass per area (LMA), light-saturated net photosynthetic rate per mass (A_{mass}), dark respiration rate, P concentration ($[P_{total}]$), nitrogen concentration, and P resorption, were measured for three pioneer and nine non-pioneer species. Leaf P was separated into five functional fractions: orthophosphate P (P_i), metabolite P (P_M), nucleic acid P (P_N), lipid P (P_L), and residual P (P_R; phosphorylated proteins and unidentified compounds that contain P).

Results LL was negatively correlated with A_{mass} and positively correlated with LMA, representing the LES. Pioneers occurred towards the short-LL end of the spectrum and exhibited higher $[P_{total}]$ than non-pioneer species, primarily associated with higher concentrations of P_i, P_N and P_L. There were no significant correlations between leaf P fractions and LL or LMA, while A_{mass} was positively correlated with the concentration of P_R.

Responsible Editor: Augusto Franco.

Supplementary Information The online version contains supplementary material available at https://doi.org/10.1007/s11104-023-06001-x.

Y. Tsujii (✉) · B. Fan · B. J. Atwell · Z. Lei · I. J. Wright
School of Natural Sciences, Macquarie University, Sydney, NSW, Australia
e-mail: yukitsuj@gmail.com

Y. Tsujii
Faculty of Science, Kyushu University, Fukuoka, Japan

Y. Tsujii · I. J. Wright
Hawkesbury Institute for the Environment, Western Sydney University, Richmond, NSW, Australia

Present Address:
Y. Tsujii
Forestry and Forest Products Research Institute (FFPRI), Tsukuba, Japan

B. Fan
College of Life Science, Northwest Normal University, Lanzhou, China

H. Lambers
School of Biological Sciences, The University of Western Australia, Perth, WA, Australia

Z. Lei
The Key Laboratory of Oasis Eco-Agriculture, Xinjiang Production and Construction Corps, Shihezi University, Shihezi, China

Z. Lei
College of Agronomy, Northwest A&F University, Yangling, China

Conclusions Allocation of leaf P to different fractions varied substantially among species. This variation was partially associated with the LES, which may provide a mechanism underlying co-occurrence of species with different ecological strategies under P limitation.

Keywords Carboxylation rate · Element cycling · Functional traits · Nutrient-use efficiency · Phosphorus deficiency · Photosynthetic P-use efficiency · Stoichiometry · Trade-off

Introduction

Phosphorus (P) is a key limiting nutrient for plant growth in many terrestrial ecosystems (Elser et al. 2007; Vitousek et al. 2010; Du et al. 2020). Because plants allocate P to vital functions that include photosynthesis, gene expression, protein synthesis, dark respiration and cell membrane structures (White and Hammond 2008; Hawkesford et al. 2023; Lambers and Oliveira 2019), P allocation among different functions relates to indicators of plant performance such as photosynthetic capacity (Hidaka and Kitayama 2013; Ellsworth et al. 2015; Mo et al. 2019) and cold tolerance (Yoshida and Sakai 1973; Willemot 1975; Yan et al. 2021). P in leaves can be chemically separated into five functional fractions: orthophosphate P (P_i), metabolite P (P_M; low-molecular-weight metabolites such as RuBP, NADP, ATP, ADP, sugar phosphates, and pyrophosphate, as well as phytate, which is strictly not a metabolite but rather, a storage compound), nucleic acid P (P_N; RNA and DNA), lipid P (P_L; phospholipids, predominantly cell membrane lipids), and residual P (P_R; phosphorylated proteins and unidentified compounds that contain P) (Chapin and Kedrowski 1983; Kedrowski 1983; Hidaka and Kitayama 2011; Yan et al. 2019). Hereafter, we describe the concentration of each leaf P fraction as $[P_i]$, $[P_M]$, $[P_N]$, $[P_L]$ and $[P_R]$; and their relative proportions per total leaf P as rP_i, rP_M, rP_N, rP_L and rP_R, respectively. Allocation of P among different functional fractions within leaves varies substantially among species (Veneklaas et al. 2012; Crous and Ellsworth 2020; Lambers 2022; Suriyagoda et al. 2023).

Leaf 'economic' traits, such as leaf dry mass per unit area (LMA), light-saturated net photosynthetic rate per unit dry mass (A_{mass}) and leaf lifespan (LL) provide a potential means to link leaf P fractions to ecological strategies. The leaf economic spectrum (LES) is an important trait-related dimension of plant ecological strategy among the world's species (Reich et al. 1997; Westoby et al. 2002; Wright et al. 2004). The LES is underpinned by a strong positive relationship between LMA and LL, and negative relationships between A_{mass} and each of these traits. Functionally, the LES involves trade-offs in resource allocation between photosynthesis and leaf structures (Chabot and Hicks 1982; Shipley et al. 2006; Lambers and Poorter 2004; Onoda et al. 2004). For example, thicker cell walls increase LMA, which is related to longer LL. Higher-LMA species tend to have a higher fraction of leaf nitrogen (N) in cell walls but a lower fraction in Rubisco, the enzyme responsible for CO_2 fixation, often leading to a lower rate of photosynthesis per unit N (i.e. photosynthetic N-use efficiency; Onoda et al. 2004 and 2017; Takahashi et al. 2004; Feng et al. 2009; Guan and Wen 2011).

Whether leaf P fractions relate to the LES is not yet clear. Cell walls contain little P (Aoyagi and Kitayama 2016). However, a trade-off in P allocation may be posited between photosynthesis and P-rich cell membrane lipids (i.e. P_L). Greater rP_L may cause reduced allocation of leaf P to photosynthesis because P_L is largely independent of photosynthetic reactions. Indeed, light-saturated net photosynthetic rate per unit area (A_{area}) is unrelated to $[P_L]$, unlike other fractions, including $[P_M]$, $[P_i]$, and $[P_R]$, which are positively related to A_{area} (Hayes et al. 2022). A negative correlation between rP_L and photosynthetic rate per unit P (photosynthetic P-use efficiency, PPUE) has been reported among broad-leaved woody species from Bornean rainforests (Hidaka and Kitayama 2013), among broad-leaved woody species from forests at early successional stages on the Tibetan Plateau (Lei et al. 2021), and within a domesticated rice variety (Hayes et al. 2022). Therefore, we expect that high rP_L is correlated with low PPUE via reduced allocation of leaf P to photosynthesis (Hypothesis 1).

There is a knowledge gap for P-limited ecosystems that are dominated by species with low concentrations of total leaf P ($[P_{total}]$), e.g., from infertile sandy soils in eastern and western Australia (Wright et al. 2001; Hayes et al. 2014), or ultrabasic soils on the slopes of Mt. Kinabalu, Borneo (Kitayama and Aiba 2002). These species often exhibit high PPUE, high LMA (Denton et al. 2007; Hidaka and Kitayama 2013; Guilherme Pereira et al. 2019), and long LL simultaneously (Denton et al. 2007; Wright et al. 2001). It is reported that the high PPUE of some Proteaceae species on low-P soils is associated with the substitution of phospholipids by galactolipids and/or sulfolipids during leaf development (Lambers et al. 2012).

Moreover, rP_L was negatively correlated with PPUE but unrelated to LMA among 10 Bornean tree species (including five species on low-P ultrabasic soils and five species on relatively high-P sedimentary soils; Hidaka and Kitayama 2013). However, the relationships between LL and leaf P fractions remain unclear.

It is also possible that variation in leaf N concentration ([N]) is coordinated with leaf P fractions. In general, [N] is positively correlated with $[P_{total}]$, with a power scaling of ~ 2/3 (Elser et al. 2010; Reich et al. 2010; Tian et al. 2018). This relationship can be considered part of the LES (Wright et al. 2005). In principle, [N] may be related to $[P_N]$ because P_N consists mainly of ribosomal-RNA (rRNA) involved in the turnover of proteins (Veneklaas et al. 2012), which account for the dominant part of leaf N despite a large fraction of leaf N is allocated to chlorophyll (Evans and Clarke 2019). Protein turnover contributes strongly to leaf dark respiration rate (Thornley and Cannell 2000), also part of the LES (Wright et al. 2004). Previous reports have found $[P_N]$ to be correlated positively with [N] among 21 Bornean woody species (Hidaka and Kitayama 2011) and across two *Banksia* species in a pot experiment (Han et al. 2021). It is also demonstrated that $[P_N]$ was positively correlated with night-time leaf respiration rate per unit area across six mangrove populations grown in a glasshouse (Yan et al. 2021). Therefore, positive correlations are expected among $[P_N]$, [N], and Rd_{mass} (Hypothesis 2). A positive correlation may also be expected between [N] and $[P_R]$ because P_R contains phosphorylated proteins (Veneklaas et al. 2012).

In this study we aimed to understand how leaf P fractions are related to leaf economic traits among 12 evergreen woody species co-occurring on P-impoverished soils. The Australian continent is an ideal model system to address this question because (1) Australian soils are for the most part extremely impoverished in P due to the geologically ancient and stable landscapes (Kooyman et al. 2017); and (2) Australian plants on P-impoverished soils have a range of strategies in response to P limitation such as: 'cluster roots' that help plants 'mine' recalcitrant P forms from the soil (Shane and Lambers 2005); sclerophylly that extends leaf lifespans and nutrient residence times, reducing uptake requirements (Beadle 1954; Wright et al. 2002); preferential allocation of P to mesophyll cells, away from the epidermis (Shane et al. 2004; Hayes et al. 2018; Guilherme Pereira et al. 2018); and near-complete resorption of P before leaf abscission (Wright and Westoby 2003; Hayes et al. 2014). We analysed the correlation patterns between leaf P fractions and key leaf economic traits, including LMA, LL, A_{mass}, carboxylation capacity per unit dry mass (V_{cmax}), dark respiration per unit dry mass (Rd_{mass}), [N], leaf N:P ratio (N:P), and PPUE among 12 common, co-occurring woody species in south-eastern Australia. The 12 species included three gap-dependent pioneer species and nine non-pioneer species, widening sampling along the LES and across different ecological strategy groups. We also quantified P resorption before leaf abscission as this strongly determines P residence time in plants (Aerts 1990; Escudero et al. 1992; Kazakou et al. 2007; Tsujii et al. 2020). P resorption was expressed both as an 'efficiency' (i.e. % withdrawn) and as a 'proficiency' (i.e. P concentration in senesced leaves, $[P_{senesced}]$), describing the degree of completion of the resorption process (Killingbeck 1996). Based on knowledge from previous studies, we proposed and tested the following three hypotheses:

Hypothesis 1 (trade-off in P allocation to photosynthesis versus lipid pools): We expected that PPUE would be negatively correlated with rP_L.

Hypothesis 2 (respiration): As protein turnover and its associated rRNA machinery is a major contributor to leaf dark respiration (Thornley and Cannell 2000), we expected that $[P_N]$ would drive variation in both [N] and Rd_{mass}.

Hypothesis 3 (resorption): On the premise that different pools of leaf P have different per-unit costs for resorption (Wright et al. 2003) – specifically, the need for hydrolysis of organic P pools would confer higher per-unit resorption costs than that for labile P pools such as P_i (Tsujii et al. 2017) – we expected that rP_i would be positively correlated with P-resorption efficiency (PRE), the percentage of P resorbed before leaf abscission (Killingbeck 1996).

Materials and methods

Study sites

The present study was carried out in the Macquarie University Ecology Reserve (33°77S, 151°12E, c. 50 m above sea level), a small patch (c. 5 ha) in Lane Cove National Park (Sydney, south-eastern Australia).

The geology of Lane Cove National Park is characterised by Hawkesbury sandstone with occasional Wianamatta shale bands. The concentration of total soil P (total soil [P]) was 78 ± 10 μg g^{-1} dry mass (mean ± SD, n = 7) (the methodology of sampling and chemical analyses is provided further below), which is much lower than the global average (570 μg P g^{-1} dry mass) (He et al. 2021) but similar to another sandstone site in Sydney (94 ± 28 μg P g^{-1} dry mass, n = 5; Wright et al. 2001). However, the concentration of soluble soil P (soluble soil [P]; Bray-1 extraction) was 6.6 ± 0.6 μg P g^{-1} dry mass (n = 5, see further below for methodology), which is higher than other sandstone sites in Sydney (on average 1.2 μg P g^{-1} dry mass; Orpheus Butler unpubl. data). At the nearest weather station (33°78S, 151°11E), mean maximum and minimum annual temperature are 22.8 and 11.2 °C (during February 1971–October 1995), while mean annual precipitation is 1157.7 mm yr^{-1} (during November 1970–February 2023; data from Bureau of Meteorology, Australian Government). The study site is characterised by native bushland vegetation with some human disturbances (e.g., bush walking). Our target species (12 species in total) included: canopy trees (c. 5–10 m tall), including *Eucalyptus haemastoma* (Myrtaceae) and *Allocasuarina littoralis* (Casuarinaceae); understorey trees and shrubs, including three *Banksia* species, *Hakea sericea and Lambertia formosa* (all Proteaceae) and *Angophora hispida* and *Leptospermum trinervium* (Myrtaceae); and gap-dependent pioneers (locally known as "disturbance specialists"), including *Dodonaea triquetra* (Sapindaceae), *Pittosporum undulatum* (Pittosporaceae), and *Acacia longifolia* (Fabaceae). *Allocasuarina littoralis* and *Acacia longifolia* have N_2-fixing root symbionts (Lawrie 1982; Rodríguez-Echeverría et al. 2009). All species are evergreen woody angiosperms.

Leaf sampling

Fully expanded outer-canopy leaves (or phyllodes for *Acacia longifolia*) were sampled from five individuals of each species during early summer (November–December 2019). Hereafter, these sampled leaves are described as green leaves. We randomly sampled healthy leaves from several branches. Green leaves included newly-expanded leaves (100% expanded) and leaves produced in the previous year or before. Green leaves were snap-frozen in liquid N_2 in the field and brought back to the laboratory at Macquarie University. The samples were freeze-dried and powdered in a wire mill (mesh size 0.08 mm, Retsch ZM200, Haan, Germany) prior to chemical analyses. Recently senesced leaves of the same trees were sampled by shaking the trees (leaves with a fully formed abscission layer easily detached). Senesced leaf samples were oven-dried at 60 °C for 48 h and powdered in the same manner.

Photosynthesis, LMA, and leaf lifespan measurements

Gas exchange measurements were performed using branch samples in parallel with leaf sampling (November–December 2019). Approximately 1 m-long branches were cut with pruning shears from 2–6 mature individuals per species (one branch per individual; on average 3.5 individuals per species) in the early morning (c. 6–8 am during daylight-saving time) to avoid high daytime air temperatures. The proximal ends of sampled branches were re-cut under tap water in a bucket and transported to the laboratory at Macquarie University. A Li-Cor LI-6800 portable photosynthesis system (LICOR, Lincoln, NE, United States) was used to measure light-saturated net photosynthesis and dark respiration. A_{area} was measured under 1800 μmol m^{-2} s^{-1} of photosynthetic photon flux density (PPFD), with reference to a recent continental-scale study across Australia (Westerband et al. 2022). Dark respiration rate per unit area (Rd_{area}) was recorded once gas exchange became stable after the light in the photosynthetic chamber was turned off (i.e. PPFD = 0 μmol m^{-2} s^{-1}). The time for dark acclimation was c. 5–30 min. Stomatal conductance to water vapour (g_{sw}) and internal CO_2 concentration in leaves (C_i) were recorded to estimate carboxylation capacity (see the following section). Leaf temperature and CO_2 concentration in the chamber were kept at 25 °C and 400 μmol mol^{-1}, respectively. LMA was used to convert area-basis rates to mass-basis rates (i.e. A_{mass} and Rd_{mass}). Arithmetic means by species (hereafter, species means) were used for this calculation because the individuals used for the gas exchange measurements often differed from those for the following LMA measurements (also from those for LL monitoring or leaf P and N analyses). Therefore, we did not have within-species error estimates for A_{mass} and Rd_{mass}.

Four to 34 leaves per individual (on average 12 leaves per individual) were collected and scanned on a flat-bed scanner (CanoScan LiDE220; Canon, Tokyo, Japan). Leaves were collected from five individuals per species during the same period (not always the same day) as the gas exchange measurements were performed (i.e. November–December 2019). The areas of the scanned leaves were measured using image analysis software (Image J; US National Institutes of Health, Bethesda, MD, USA). The scanned leaves were oven-dried at 60 °C for 48 h and their dry mass determined to calculate LMA. The area of needle leaves (i.e. the leaves of *Hakea sericea* and *Allocasuarina littoralis*) was adjusted upwards by π/2 on the assumption of circular cross-sections (Wright and Westoby 2002).

Leaf censuses were conducted to estimate LL for five individuals per species following the procedure of Wright et al. (2002). The individuals used for the LL monitoring did not always correspond to those for the LMA measurement or chemical analyses. Five age-sequences of leaves were randomly selected per individual in late 2019 (in total 25 sequences per species). For *Acacia longifolia*, in total 25 branches were chosen across six individuals due to the limited replications within individuals. The number of leaves was counted along the sequence of leaf age from the youngest leaf (> 25% expanded) on the shoot top to the oldest leaf on the same or older ordered branch, or sometimes on the stem. On average, 178 leaves were counted per sequence (13–772 leaves per sequence). Wires with plastic tags were used to mark each branch (or stem). Six months later, the remaining leaves on the same branch or stem were counted and new sequences with newly-expanded leaves were marked. This census was repeated six months later (i.e. the total monitoring period was 1 year). The leaf census of *D. triquetra* was conducted every three months because of short LL (often less than six months). LL was defined as the inverse of leaf turnover rate. We estimated average LL across the two census periods. Leaf turnover rate during each census period was calculated by Eq. 1.

$$\text{Leaf turnover rate } (\text{year}^{-1}) = \left\{\left(L_{d1} - L_{d2}\right)/L_{d1}\right\}/\left\{\left(d_2 - d_1\right)/365.25\right\} \quad (1)$$

where L_{d1} and L_{d2} represent the number of leaves at the start date (d_1) and the end date (d_2) of census, respectively. One year was defined as 365.25 days.

Estimation of carboxylation capacity

Carboxylation capacity at 25 °C ($V_{cmax\ area}$; on an area basis) was estimated by the one-point method (De Kauwe et al. 2016). In this estimation, day respiration rate (i.e. non-photorespiratory CO_2 evolution in the light) was assumed as 1.5% of $V_{cmax\ area}$. The Michaelis constants for CO_2 and O_2 and the CO_2 compensation point were estimated using the equations provided by Bernacchi et al. (2001) and Crous et al. (2013), respectively. LMA was used to convert area-basis rates to mass-basis rates (i.e. V_{cmax}).

Soil sampling

In June 2020, seven soil cores (3 cm diameter and 0–15 cm depth beneath the litter layer) were randomly sampled in the ecology reserve, taken to the laboratory, and sieved with 1.18-mm mesh. The sieved soils were air-dried prior to chemical analyses.

Leaf P fraction, total leaf P and N, and soil total and soluble P analyses

Five chemical fractions in green leaves (i.e. P_i, P_M, P_N, P_L, and P_R) were determined by the sequential extraction methodology of Chapin and Kedrowski (1983) and Kedrowski (1983), with modifications by Hidaka and Kitayama (2011) and further by Yan et al. (2019). Briefly, 50 mg of powdered sample was extracted with 1 mL of chloroform–methanol-formic acid (12:6:1 v/v/v; CMF) in a 2-mL tube (tube 1) for 30 s. After being centrifuged, the supernatant was transferred into a new 15-mL tube (tube 2). This procedure was repeated three times (in total 3 mL of CMF). The pellet in the tube 1 was further extracted with 1.26 mL of chloroform–methanol-water (1:2:0.8 v/v/v; CMW) for 30 s. The extract in

the tube 1 was transferred into tube 2. This extraction was repeated three times. An aliquot of 1.9 mL of chloroform-washed water was added to tube 2, mixed by inverting, and centrifuged to separate into a lipid-rich organic bottom layer and an aqueous upper layer. The lipid-rich bottom layer was transferred to a Kjeldahl tube labelled 'P_L'. The remaining aqueous layer with precipitates was transferred to another tube (tube 3). The pellet in tube 1 was vacuum-dried and then extracted with 1 mL of 85% (v/v) methanol for 30 s. The extract in tube 1 was transferred to tube 3. An aliquot of 1 mL of cold 5% (v/v) trichloroacetic acid (TCA) was added to the residual pellet in tube 1, and extracted for 1 h (1 min shaking, with 9 min intervals). The extract was transferred into tube 3. This extraction was repeated twice. The extract in tube 3 contains P_i and P_M and was labelled '$P_i + P_M$'. The pellets after the cold-TCA extraction (tube 1) were extracted three times with hot-TCA (2.5% w/v) at 95 °C (1 mL × 3) for one hour each. The hot-TCA extractant and the remaining residue in the tube 1 corresponded to P_N and P_R, respectively. Samples were kept at 4ºC during the experiments, except for the hot-TCA extraction. An Eppendorf shaker (Thermomixer, at 1400 rpm) was used for the cold extractions. All solid–liquid separations were accomplished by centrifugation with 1028 × g at 4ºC for 10 min. We accepted the data with > 90% of recovery rates (i.e. the percentage of the sum of [P] in the fractions per [P_{total}]).

[P_M] was determined by subtracting [P_i] from the concentration of the composite fraction of P_i and P_M. During the P_i assay, the activated-charcoal filtering procedure by Dayrell et al. (2022) was used to remove interferences such as turbidity, colouration, and precipitation. Briefly, 25 mg of powdered sample was extracted with 0.5, 0.5, and 0.75 ml of 1% (v/v) acetic acid by shaking at 1400 rpm for 15 s, with 5 min intervals. After the homogenate was centrifuged at 21,000 × g for 15 min, 1.6 mL of the supernatant was transferred to the 2 mL tube with 16 mg acid-washed activated charcoal. The tube was shaken for 30 s, and then the solution with activated charcoal in the tube was filtered through a syringe filter (0.45 µm, diameter = 25 mm). The same procedure was applied also for the standard solutions of P_i. Sample temperature was always kept at 4 °C. P_i in the filtered solution was quantified by the molybdenum blue method (Murphy and Riley 1962) using a spectrophotometer (UV-mini 1240, Shimadzu Co., Kyoto, Japan). The detection wavelength was set at 712 nm to reduce the colour interference by yellow organic matters (Tiessen and Moir 1993).

Powdered leaves and the dried lipid fraction were digested with 2.5 mL of concentrated H_2SO_4 and 1 mL of 30% H_2O_2 at 360 °C for 3 h. The liquid samples (i.e. cold- and hot-TCA extractants) and wet solid samples (i.e. the residual fraction) were digested with 2.5 mL H_2SO_4 for 3 h, after water in the samples was evaporated by a gradual increase in temperature up to 150 °C. P concentrations in the digests were determined by the molybdenum blue method (Murphy and Riley 1962), with 882 nm as the detection wavelength. Leaf [N] was determined by the combustion method using a Vario MICRO cube elemental analysers (Elementar Analysensysteme GmbH, Hanau, Germany).

Total soil [P] was determined by the molybdenum blue method (Murphy and Riley 1962) after digestion with H_2SO_4 and $HClO_4$ (Olsen and Sommers 1982). Regarding soil soluble [P], 25 ml of Bray-I solution was added to 3.55 g of air-dried soils and shaken by hand for 30 s. Orthophosphate in the Bray-I extract was quantified by the molybdenum blue method (Murphy and Riley 1962), with 712 nm as the detection wavelength. The data for total and soluble soil [P] are provided in the site description section above.

Calculations of PPUE and PRE

PPUE was calculated as A_{mass} per [P_{total}]. PRE was calculated by Eq. 2. Mass loss during senescence was corrected by a mass loss correction factor (MLCF = 0.78; the global average of evergreen angiosperms) (Vergutz et al. 2012).

$$\mathrm{PRE}(\%) = \left\{1 - \left[P_{senesced}\right] \times \mathrm{MLCF} / \left[P_{total}\right]\right\} \times 100(\%) \quad (2)$$

Statistical analyses

One-way ANOVA with Tukey's HSD post hoc test was used to test for trait differences among species, with individuals as the units of replication. Pearson's correlation tests quantified relationships among leaf P fractions and leaf economic traits. In the correlation

tests, species means were used as the units of replication. Exceptionally, medians by species were calculated for LL to avoid potential bias from outliers of some individuals with unnaturally long LLs (> 10 years; see Fig. 2). [$P_{senesced}$] was log-transformed before the correlation test to normalise the data. We set the significance level at $P < 0.05$.

The same analyses were also applied to area-basis data to check whether the basis of expression (mass vs area) made a difference to the main trends. The area-based contents of leaf P and N were calculated as the product of species-mean mass-based concentration data and species-mean LMA data. Therefore, there is no replication within species. Hereafter, we describe the area-based contents of total leaf P, N, P_i, P_M, P_N, P_L, and P_R, as $P_{total\ area}$, N_{area}, $P_{i\ area}$, $P_{M\ area}$, $P_{N\ area}$, $P_{L\ area}$, and $P_{R\ area}$, respectively.

All statistical analyses were done in R version 3.0.1 (R Core Team 2020). The ggplot2 package (Wickham 2016) was used to visualise data.

Results

Variation in the concentration of leaf total P and P fractions

Mean [P_{total}] significantly varied among the species, from 0.26 to 0.74 mg g^{-1} dry mass (Fig. 1, $P < 0.01$), with the lowest value in the sclerophyllous shrub *Hakea sericea* and the highest in a pioneer, *Pittosporum undulatum*. Indeed, all three pioneer species exhibited higher [P_{total}] than the non-pioneer species. The concentration of each P fraction also varied significantly among species (Fig. 2, $P < 0.01$). [P_R] varied the least among the species (c. two-fold; 0.03–0.06 mg g^{-1}, Fig. 2d), while [P_i] and [P_M] varied the most (c. five-fold; 0.05–0.24 and 0.02–0.10 mg g^{-1}, respectively, Fig. 2a and b), with variation in [P_N] and [P_L] intermediate (c. three-fold among species: 0.06–0.22 and 0.07–0.20 mg g^{-1}, respectively, Fig. 2c and d). Among families, the species in the Proteaceae and Casuarinaceae exhibited the lowest [P_L] (the fraction including cell membranes; 0.07–0.09 mg g^{-1}). Proteaceae generally had low [P_N] (0.08–0.13 mg g^{-1}). The three pioneer species stood out in having higher [P_N] (0.18–0.22 mg g^{-1}) and [P_L] (0.14–0.20 mg g^{-1}) than non-pioneer species. [P_M] (including substrates and products of photosynthetic enzymes) varied widely between all species combined. High [P_i] was found in a non-pioneer species, *Eucalyptus haemastoma*, as well as pioneer species. No clear differences in [P_R] were found among families.

Next, we considered the 'relative' P allocation to different pools (Fig. 3). On average, the largest relative fraction was rP_N (28%), followed by rP_i and rP_L (27 and 24%). The smallest fractions were rP_R and rP_M (9 and 12%, respectively). Most notably, rP_N and rP_L varied the least among species (c. 1.5-fold;

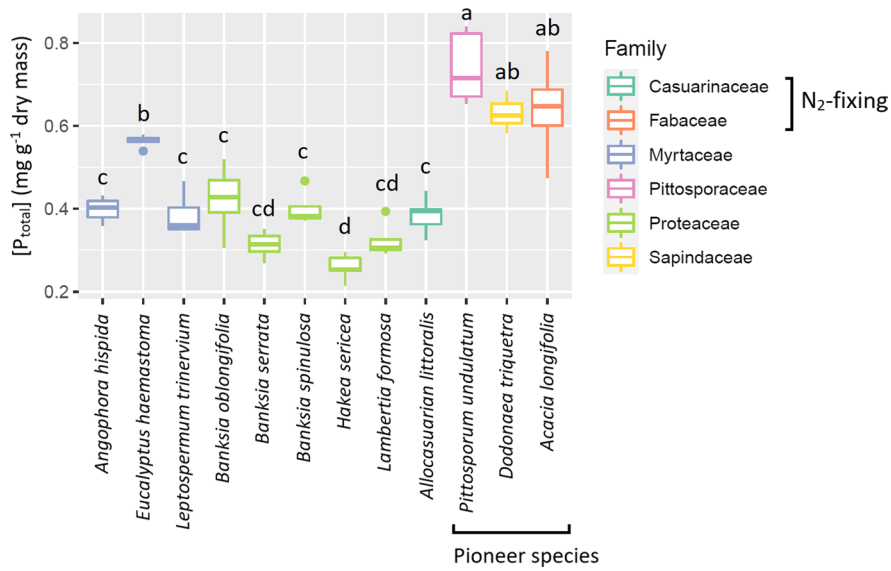

Fig. 1 Box plots showing [P_{total}] for 12 Australian woody species. The colours of each box pertain to families. The central box shows the interquartile range and median by species; the whiskers extend 1.5 times the interquartile range or to the most extreme value. Pairwise significant differences among species are shown as different letters (Tukey HSD, $P < 0.05$)

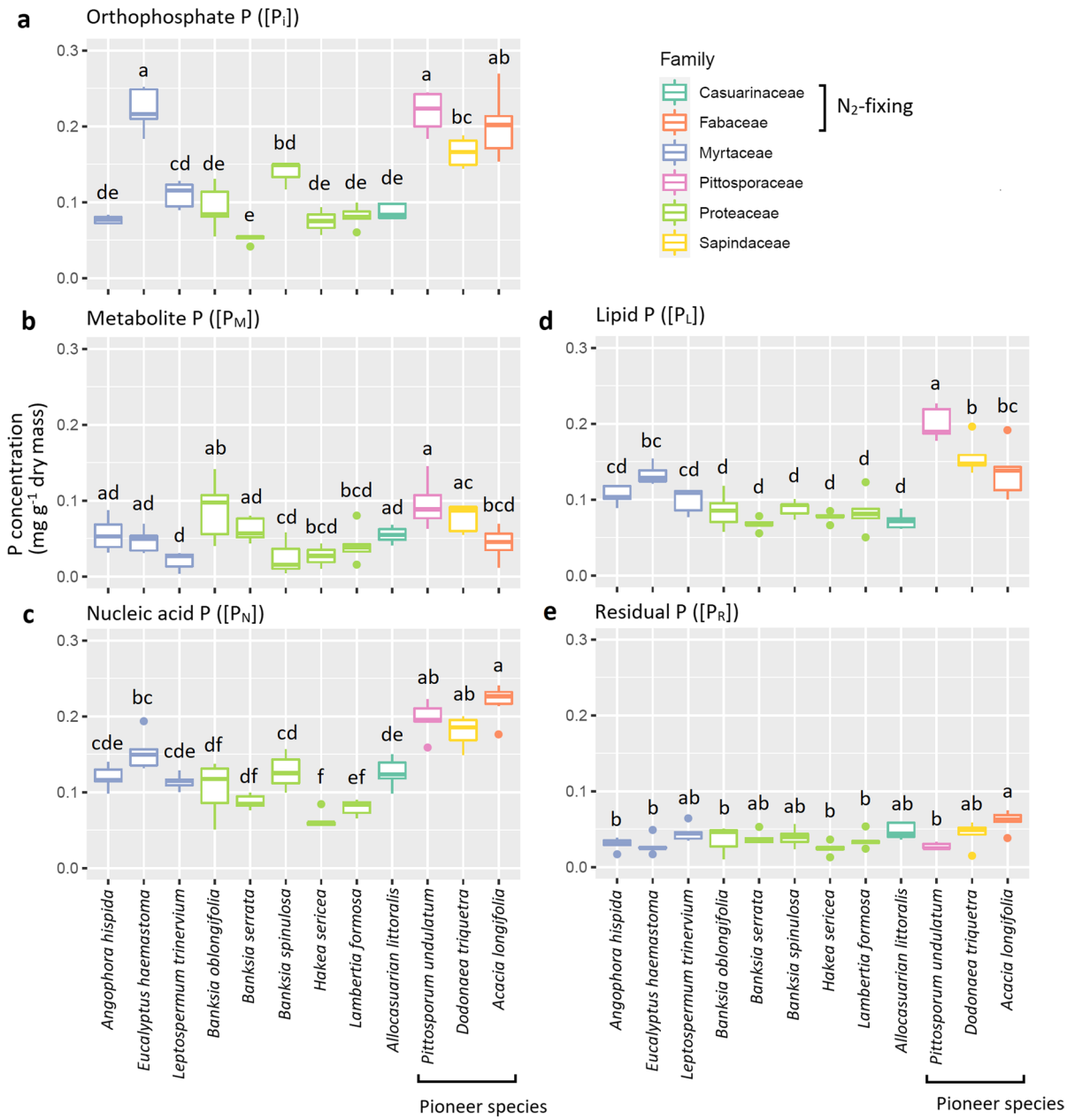

Fig. 2 Box plots showing the concentrations of each P fraction for 12 Australian woody species. The colours of each box pertain to families. The central box shows the interquartile range and median by species; the whiskers extend 1.5 times the interquartile range or to the most extreme value. Pairwise significant differences among species are shown as different letters (Tukey HSD, $P < 0.05$)

22–33% and 19–27%, respectively, Fig. 3c and d), while rP_M and rP_R varied the most (c. four-fold; 5–22% and 3–12%, respectively, Fig. 3b and e). rP_i varied c. two-fold (17–38%, Fig. 3a). No consistent patterns were apparent between families or within growth forms.

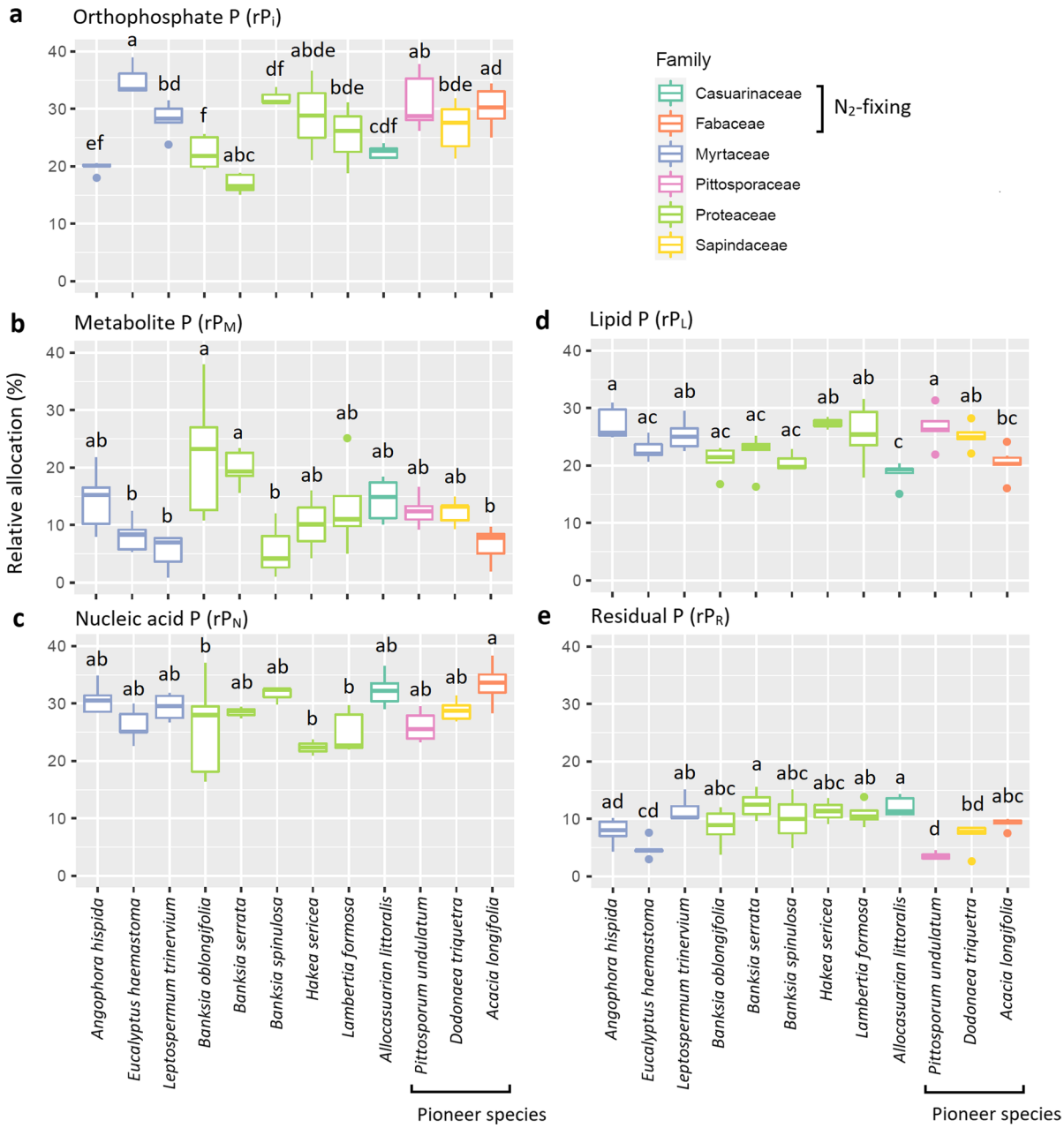

Fig. 3 Box plots showing the relative allocation to each P fraction for 12 Australian woody species. The colours of each box pertain to families. The central box shows the interquartile range and median by species; the whiskers extend 1.5 times the interquartile range or to the most extreme value. Pairwise significant differences among species are shown as different letters (Tukey HSD, $P < 0.05$)

Variation in leaf economic traits

Leaf economic traits significantly varied among the species (Fig. 4; $P < 0.05$). LMA varied 2.6-fold among species, with the lowest mean LMA in the pioneer species *Dodonaea triquetra* (141 g m^{-2}) and the highest in *Eucalyptus haemastoma* (362 g m^{-2}) (Fig. 4a). LL varied > six-fold among species, from 0.48 year in *Dodonaea triquetra* to 3.2 year in *Banksia oblongifolia* (Fig. 4b). A_{mass} varied > three-fold,

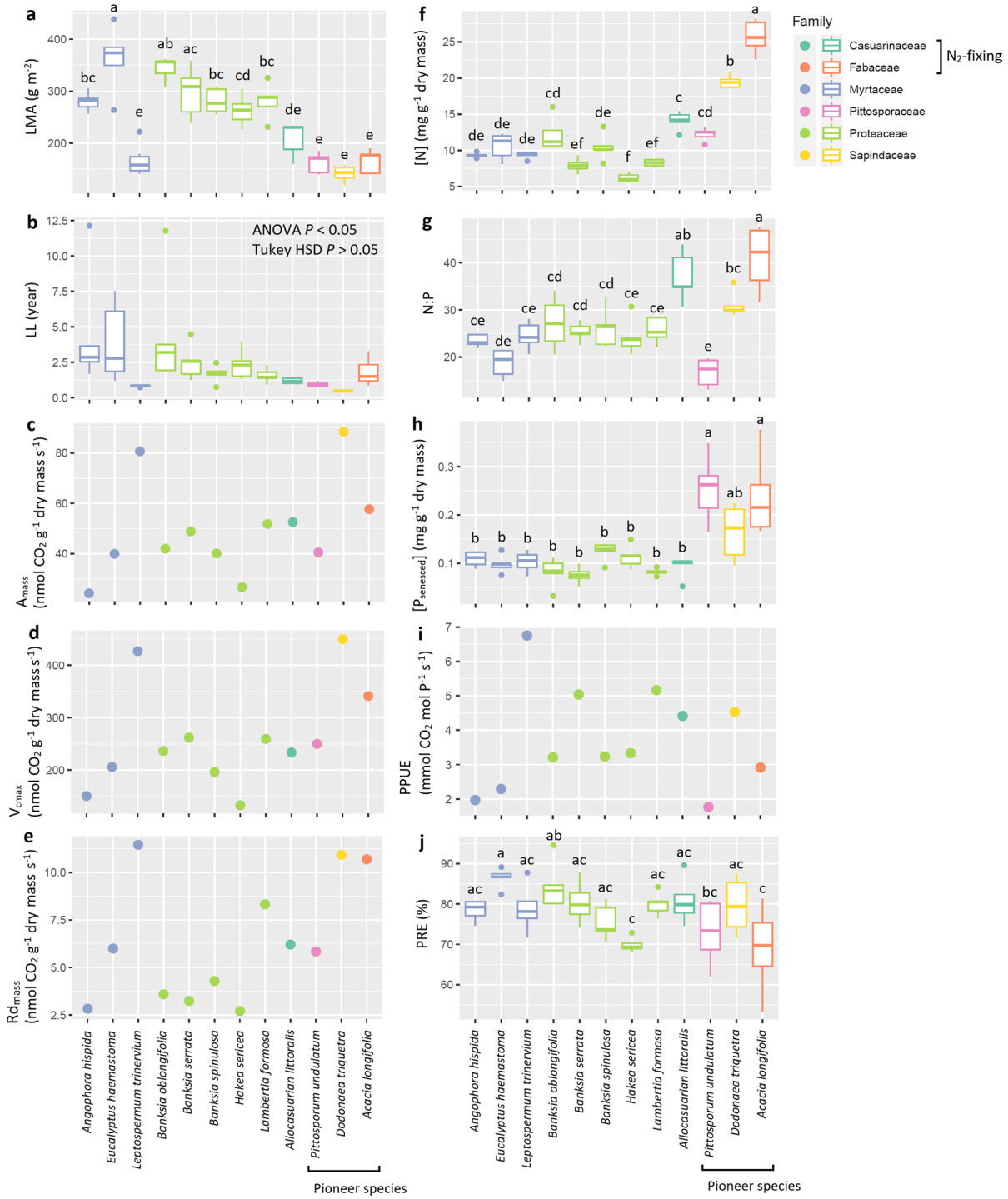

Fig. 4 Box plots showing leaf economic traits for 12 Australian woody species. The colours of each box pertain to families. The central box shows the interquartile range and median by species; the whiskers extend 1.5 times the interquartile range or to the most extreme value. For A_{mass} and Rd_{mass} (panels C and D), one data point is provided per species (see Methods). Different letter indicates significant differences among species (Tukey HSD, $P < 0.05$) for each trait

from 24.4 nmol CO_2 g^{-1} s^{-1} (*Angophora hispida*) to 88.5 nmol CO_2 g^{-1} s^{-1} (*Dodonaea triquetra*; Fig. 4c). V_{cmax} varied > three-fold, from 133 nmol CO_2 g^{-1} s^{-1} (*Hakea sericea*) to 449 nmol CO_2 g^{-1} s^{-1} (*Dodonaea triquetra*; Fig. 4d). Rd_{mass} varied > four-fold, from 2.7 nmol CO_2 g^{-1} s^{-1} in *Hakea sericea* to 11.5 nmol CO_2 g^{-1} s^{-1} in *Leptospermum trinervium* (Fig. 4e).

[N] varied > four-fold among species, from 6.2 mg g^{-1} dry mass (*Hakea sericea*) to 25.7 mg g^{-1} dry mass in the N_2-fixing pioneer, *Acacia longifolia* (Fig. 4f). N:P varied < three-fold, with the lowest value in a pioneer, *Pittosporum undulatum* (16.5) and the highest in the N_2-fixing pioneer, *Acacia longifolia* (40.3) (Fig. 4g). [$P_{senesced}$] varied > three-fold from 0.08 mg g^{-1} (*Banksia serrata*) to 0.25 mg g^{-1} in the pioneer, *Pittosporum undulatum* (Fig. 4h).

PPUE varied c. four-fold among the species (1.7–6.7 mmol CO_2 mol P^{-1} s^{-1}), with the lowest PPUE in *Pittosporum undulatum* and the highest PPUE in a non-pioneer, *Leptospermum trinervium* (Fig. 4i). PRE varied from 66% in *Hakea sericea* to 86% in *Eucalyptus haemastoma* (Fig. 4j; both non-pioneer species).

Correlation patterns among leaf P fractions and economic traits

The results from correlation tests are summarised in Table 1. First, we report correlation patterns between leaf P fractions and between economic traits, followed by those of leaf P fractions to LMA, LL, A_{mass} (Hypothesis 1); those to Rd_{mass} and [N] (Hypothesis 2); and those to resorption (Hypothesis 3).

Correlations between leaf P fractions

[P_{total}] was significantly positively correlated with each of [P_i], [P_N] and [P_L] (r = 0.91–0.95, $P < 0.01$); however, it was unrelated to [P_M] or [P_R] (r = 0.19–0.54, $P = 0.07$–0.56). Significant positive correlations were found among [P_i], [P_N] and [P_L] (r = 0.83–0.87, $P < 0.01$). [P_M] or [P_R] was unrelated to the other P fractions.

Considering relative P allocations, no significant correlations were found among P fractions, except for a negative correlation between rP_i and rP_M (r = -0.75, $P < 0.01$). However, rP_i and rP_M were not statistically independent as [P_M] was estimated as the difference between P_i and the composite fraction of P_M and P_i. [P_{total}] was correlated only with rP_R (r = -0.82, $P < 0.01$).

Correlations between leaf economic traits

Correlations among leaf economic traits were much as expected. LMA was positively correlated with LL (r = 0.88, $P < 0.01$). LL was negatively correlated with both A_{mass} and Rd_{mass} (r = -0.72 and -0.76, respectively; both $P < 0.01$). A_{mass} and Rd_{mass} were themselves positively correlated (r = 0.87, $P < 0.01$). V_{cmax} showed the same pattern as A_{mass}. Species with high leaf [P_{total}] also had higher [N] and [$P_{senesced}$] (r = 0.68 and 0.83, $P < 0.05$ and < 0.01, respectively). [N] was positively correlated with Rd_{mass}, and [$P_{senesced}$] (r = 0.60, and 0.65, $P < 0.05$, and < 0.05, respectively). Higher-LMA species had lower [$P_{senesced}$] (r = -0.70, $P = 0.01$).

Correlations of leaf P fractions with LMA, LL, A_{mass}, and PPUE (hypothesis 1)

Leaf P fractions were statistically independent of LMA or LL (r = -0.55–0.37, $P = 0.06$–0.91). A_{mass} and V_{cmax} were significantly positively correlated with [P_R] (r = 0.62 and 0.63, $P < 0.05$; see Fig. 5a for A_{mass}) but unrelated to [P_M] (r = 0.00 and 0.08, $P = 1.00$ and 0.80, respectively), despite this fraction containing substrates and products of photosynthetic enzymes. PPUE was significantly positively correlated with rP_R (r = 0.70, $P < 0.05$; Fig. 5b) but, unexpectedly, unrelated to rP_M (r = -0.03, $P = 0.92$) or rP_L (including cell membranes; r = -0.07, $P = 0.84$).

Correlations of leaf P fractions to Rd_{mass} and to [N] (hypothesis 2)

As predicted, [P_N] was positively correlated with [N] (r = 0.83, $P < 0.01$). Higher Rd_{mass} was positively associated with [N] (r = 0.60, $P < 0.05$). [P_R] was correlated with Rd_{mass} and [N] (r = 0.65 and 0.76, $P < 0.05$ and < 0.01, respectively).

Table 1 The results from Pearson's correlation tests between the concentrations of leaf P fractions and leaf economic traits (above diagonal) and between the relative allocations to each P fraction and leaf economic traits (below diagonal) for 12 Australian woody species. * $P < 0.05$. † [$P_{senesced}$] was log-transformed to normalise the distribution

		P_i	P_M	P_N	P_L	P_R	[P_{total}]	LMA	LL	A_{mass}	V_{cmax}	Rd_{mass}	[N]	N:P	[$P_{senesced}$]†	PPUE	PRE
P_i	r		0.26	0.86*	0.87*	0.08	0.91*	-0.31	-0.33	0.16	0.25	0.40	0.53	-0.14	0.76*	-0.48	-0.16
	P		0.41	0.00	0.00	0.80	0.00	0.32	0.30	0.62	0.43	0.20	0.07	0.66	0.00	0.11	0.62
P_M	r	-0.75*		0.36	0.51	-0.17	0.54	-0.07	0.02	0.00	0.08	-0.14	0.24	-0.09	0.24	-0.38	0.24
	P	0.01		0.24	0.09	0.60	0.07	0.84	0.94	1.00	0.80	0.67	0.45	0.77	0.44	0.22	0.45
P_N	r	-0.14	-0.25		0.83*	0.43	0.95*	-0.55	-0.43	0.32	0.43	0.51	0.83*	0.24	0.84*	-0.40	-0.26
	P	0.66	0.43		0.00	0.16	0.00	0.06	0.16	0.31	0.16	0.09	0.00	0.46	0.00	0.19	0.42
P_L	r	0.03	-0.10	-0.56		-0.06	0.94*	-0.50	-0.43	0.21	0.33	0.38	0.47	-0.25	0.83*	-0.46	-0.23
	P	0.92	0.75	0.06		0.86	0.00	0.10	0.17	0.52	0.29	0.22	0.12	0.43	0.00	0.13	0.48
P_R	r	-0.52	0.08	0.18	-0.28		0.19	-0.50	-0.42	0.62*	0.63*	0.65*	0.76*	0.87*	0.23	0.39	-0.18
	P	0.08	0.81	0.59	0.38		0.56	0.10	0.18	0.03	0.03	0.02	0.00	0.00	0.46	0.22	0.57
[P_{total}]	r	0.49	-0.22	0.21	-0.01	-0.82*		-0.47	-0.39	0.28	0.40	0.44	0.68*	0.00	0.82*	-0.46	-0.14
	P	0.11	0.49	0.52	0.97	0.00		0.12	0.20	0.38	0.20	0.16	0.01	0.99	0.00	0.13	0.65
LMA	r	-0.06	0.37	-0.37	-0.16	0.04	-0.47		0.88*	-0.63*	-0.67*	-0.69*	-0.55	-0.33	-0.70*	-0.25	0.54
	P	0.84	0.23	0.24	0.63	0.91	0.12		0.00	0.03	0.02	0.01	0.06	0.29	0.01	0.44	0.07
LL	r	-0.21	0.44	-0.25	-0.09	0.01	-0.39	0.88*		-0.72*	-0.69*	-0.76*	-0.40	-0.22	-0.52	-0.41	0.32
	P	0.51	0.15	0.43	0.78	0.98	0.20	0.00		0.01	0.01	0.00	0.20	0.49	0.08	0.18	0.31
A_{mass}	r	0.03	-0.21	0.29	-0.11	0.12	0.28	-0.63*	-0.72*		0.97*	0.87*	0.47	0.37	0.16	0.69*	0.13
	P	0.93	0.51	0.36	0.73	0.72	0.38	0.03	0.01		0.00	0.00	0.12	0.23	0.63	0.01	0.69
V_{cmax}	r	0.04	-0.21	0.29	-0.05	0.01	0.40	-0.67*	-0.69*	0.97*		0.89*	0.54	0.34	0.28	0.59*	0.04
	P	0.90	0.52	0.35	0.88	0.98	0.20	0.02	0.01	0.00		0.00	0.07	0.27	0.37	0.04	0.90
Rd_{mass}	r	0.30	-0.49	0.31	-0.03	-0.04	0.44	-0.69*	-0.76*	0.87*	0.89*		0.60*	0.38	0.39	0.48	-0.09
	P	0.34	0.10	0.32	0.92	0.90	0.16	0.01	0.00	0.00	0.00		0.04	0.23	0.22	0.11	0.79
[N]	r	0.18	-0.20	0.58*	-0.41	-0.24	0.68*	-0.55	-0.40	0.47	0.54	0.60*		0.71*	0.65*	-0.15	-0.27
	P	0.58	0.54	0.05	0.18	0.45	0.01	0.06	0.20	0.12	0.07	0.04		0.01	0.02	0.65	0.39
N:P	r	-0.26	0.01	0.62*	-0.64*	0.45	0.00	-0.33	-0.22	0.37	0.34	0.38	0.71*		0.10	0.23	-0.19
	P	0.41	0.97	0.03	0.03	0.14	0.99	0.29	0.49	0.23	0.27	0.23	0.01		0.76	0.47	0.55
[$P_{senesced}$]†	r	0.46	-0.44	0.24	0.15	-0.55	0.82*	-0.70*	-0.52	0.16	0.28	0.39	0.65*	0.10		-0.44	-0.68
	P	0.13	0.15	0.45	0.63	0.06	0.00	0.01	0.08	0.63	0.37	0.22	0.02	0.76		0.15	0.02
PPUE	r	-0.31	-0.03	0.05	-0.07	0.70*	-0.46	-0.25	-0.41	0.69*	0.59*	0.48	-0.15	0.23	-0.44		0.20
	P	0.33	0.92	0.87	0.84	0.01	0.13	0.44	0.18	0.01	0.04	0.11	0.65	0.47	0.15		0.53
PRE	r	-0.17	0.43	-0.11	-0.24	-0.09	-0.14	0.54	0.32	0.13	0.04	-0.09	-0.27	-0.19	-0.68*	0.20	
	P	0.61	0.16	0.74	0.46	0.79	0.65	0.07	0.31	0.69	0.90	0.79	0.39	0.55	0.02	0.53	

Correlations between leaf P fractions and P resorption (hypothesis 3)

$[P_{senesced}]$ (i.e. P-resorption proficiency) was positively correlated with $[P_i]$, $[P_N]$, and $[P_L]$ (r = 0.76–0.84, $P < 0.01$). PRE was not significantly correlated with the relative allocation to each P fraction ($P = 0.16$–0.79), in contrast to our hypothesis 3.

Area basis data

A_{area} varied > twofold, from 6.6 µmol CO_2 m^{-2} s^{-1} (*Pittosporum undulatum*) to 15.6 µmol CO_2 m^{-2} s^{-1} (*Banksia serrata*; Fig. S1a). $V_{cmax\ area}$ varied > twofold, from 34.9 µmol CO_2 m^{-2} s^{-1} (*Hakea sericea*) to 81.2 µmol CO_2 m^{-2} s^{-1} (*Banksia oblongifolia*; Fig. S1b). Rd_{area} varied > three-fold, from 0.7 µmol CO_2 m^{-2} s^{-1} in *Hakea sericea* to 2.3 µmol CO_2 m^{-2} s^{-1} in *Lambertia formosa* (Fig. S1c). There were no significant variations among species in either A_{area}, $V_{cmax\ area}$, or Rd_{area} (Figs S1a–c; $P = 0.05$–0.06).

$P_{total\ area}$ varied > three-fold among species, from 64.4 to 204.1 mg m^{-2} (Fig. S1d), with the lowest value in the low-LMA and low-$[P_{total}]$, *Leptospermum trinervium* and the highest value in the high-LMA and high $[P_{total}]$, *Eucaluyptus haemastoma*. N_{area} varied c. threefold among species, ranging from 1563 mg m^{-2} in the low-LMA and low [N], *Leptospermum trinervium* to 4633 mg m^{-2} in a N_2-fixing, *Allocasuarina littoralis* (Fig. S1e). As for leaf P fraction, $P_{N\ area}$ and $P_{L\ area}$ varied the least among species (c. twofold; 19.0–55.6 and 16.5–48.3 mg m^{-2}, Figs S1h and i), while $P_{M\ area}$ varied the most (> eightfold; 3.4–30.4 mg m^{-2}, Fig. S1g), followed by $P_{i\ area}$ and $P_{R\ area}$ (c. fivefold and > threefold; 15.5–80.5 and 4.4–15.6 mg m^{-2} respectively, Figs S1f and j). There were no systematic differences in the area-basis leaf P fractions among families or growth forms.

Correlation patterns among these area-basis traits were similar to those among mass-basis traits (Table S1). Exceptionally, Rd_{area} was not related to leaf P fractions although Rd_{mass} was significantly related to $[P_R]$.

Discussion

Among all 12 study species, LL was correlated negatively with A_{mass} and Rd_{mass}. LL was also positively correlated with LMA, representing the LES (Reich

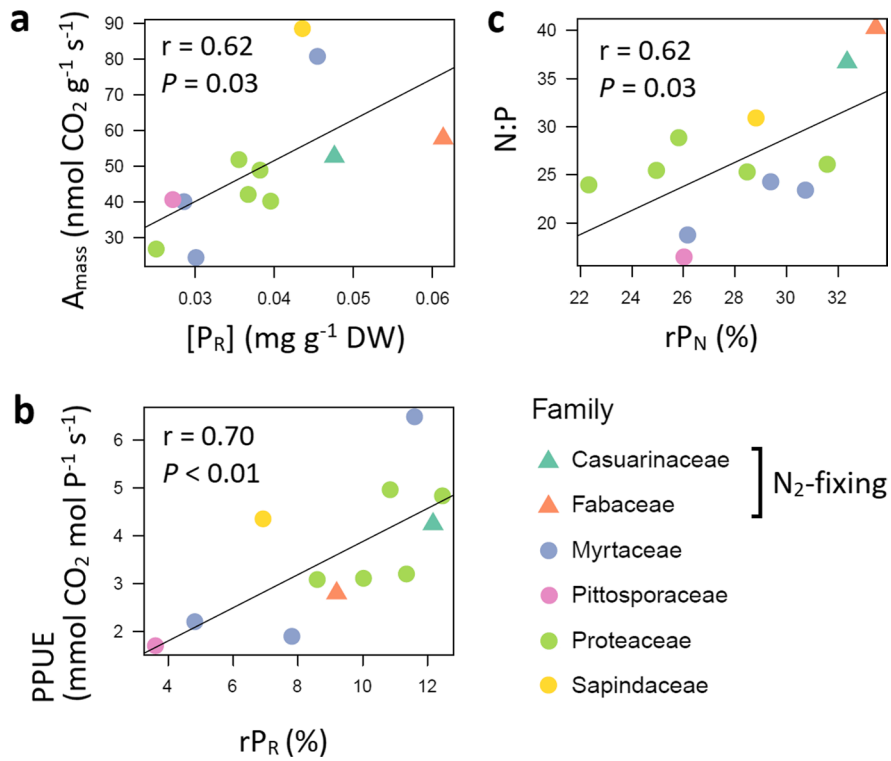

Fig. 5 Correlations between A_{mass} and $[P_R]$ (panel a); between PPUE and rP_R (panel b); and between N:P and rP_N (panel c) among 12 Australian woody species. Solid lines indicate significant correlations ($P < 0.05$). Different colours pertain to different families. Triangles and circles correspond to N_2-fixing species and non-fixing species, respectively

et al. 1997; Westoby et al. 2002; Wright et al. 2004) that spanned low-LMA pioneer species to non-pioneers with high LMA. Differences in the concentrations of leaf P fractions were found between the ecological strategy groups, with higher [P_i], [P_N] and [P_L] in pioneer species; these species showed notably high [$P_{senesced}$]. Considering P allocations as a proportion of [P_{total}], the N_2-fixing species exhibited higher rP_N than the non-fixing species. This is in agreement with a previous report for a pioneer Fabaceae species in Western Australia (Yan et al. 2019), presumably reflecting high capacities for protein synthesis. Presence of N_2-fixning species was involved in the positive correlation between rP_N and N:P (Fig. 5c), with no significant pattern when analysed excluding the N_2-fixing species ($r=0.54$, $P=0.22$, data not shown). Therefore, growth strategy and N_2-fixation capacity described the association between the LES and leaf P fractions. In the following sections, we discuss how leaf P fractions are coordinated with the LES in relation to (1) trade-offs in P allocation; (2) respiration; and (3) P resorption.

Trade-offs in P allocation (Hypothesis 1)

Hypothesis 1 is based on the premise that there is a trade-off in P allocation between photosynthesis and phospholipid-rich cell membranes. rP_L is negatively related to PPUE (Hidaka and Kitayama 2013; Hayes et al. 2022; Lei et al. 2021). In contrast to these previous studies, here PPUE was unrelated to rP_L, this implies that there was no trade-off in P allocation to photosynthesis versus P_L among our study species. One explanation comes from the Proteaceae, in which low expression of rRNA may be involved in high PPUE (Sulpice et al. 2014) as well as membrane phospholipids with low-P galactolipids and/or sulfolipids may substitute for high-P phospholipids (Lambers et al. 2012). Indeed, many Proteaceae species studied here exhibited low [P_N] and [P_L]. In addition, the non-significant link between [P_{total}] and LMA ($r=-0.47$, $P=0.12$) in this dataset might cause the decoupling between relative P fractions and the LES.

Species with higher A_{mass} had higher [P_R]; species with higher PPUE had higher rP_R. This suggests that P_R reflects some aspect of photosynthetic P metabolism, perhaps via the phosphorylation of photosynthetic proteins (Veneklaas et al. 2012). It was therefore surprising that [P_M] was *not* correlated with A_{mass}, even though this fraction captures the P incorporated into soluble photosynthetic reactants. This may be because P_M included phytates, that may be present as storage compounds, rather than metabolically active compounds (Lambers 2022), or involved in cellular signalling (Kumar et al. 2021). Polyphosphate, a storage form of inorganic P reported for *Banksia ornata* in an Australian heathland (Jeffrey 1964), might be also contained in P_M (and perhaps also in P_N and/or P_R) because it can be partly extracted by 8% cold-TCA solution (Miyachi and Tamiya 1961). Supporting the suggestion that inorganic P storage might be elevated at the expense of P_M, there was a negative correlation between rP_M and rP_i implying that partitioning among P storage pools such as P_i (stored largely in vacuoles; White and Hammond 2008), polyphosphate, and phytate, differs among species. Detailed chemistry of P_M and P_i needs to address this possibility, because the P-fractionation method that we used does not distinguish metabolically active forms from storage forms, particularly in P_M (Lambers 2022).

We estimated V_{cmax} (or $V_{cmax\ area}$) to allow for potential stomatal limitation in photosynthesis. There was a significant positive correlation between g_{sw} and A_{area} ($r=0.91$, $P<0.01$; Fig. S2), implying that stomatal limitation constrained A_{area}. However, the correlations of leaf P fractions with V_{cmax} (or $V_{cmax\ area}$) were similar to those with A_{mass} (or A_{area}). This suggests that the correlations between leaf P fractions and A_{mass} (or A_{area}) were independent of stomatal limitation.

Respiration (Hypothesis 2)

As we expected, [N] was more tightly correlated with [P_N] than with [P_{total}] or other P fractions. This may be because the synthesis of rRNA involves the turnover of proteins. P_R may correlate with the degree of phosphorylation of photosynthetic proteins (Veneklaas et al. 2012) which is the reason why [P_R] and Rd_{mass} were correlated. However, it should be noted that Rd_{area} was not correlated with $P_{R\ area}$. This suggests that the Rd_{mass}–[P_R] relationship partially resulted from covariation of each trait with LMA.

P-resorption patterns (Hypothesis 3)

PRE was independent of P-allocation patterns. This contradicts Hypothesis 3 but accords with a previous study for Bornean woody species (Tsujii et al. 2017), in which higher PREs involved greater degradation of organic P (i.e. P_N, P_L, and P_R). Similarly, our target

species must have hydrolysed substantial organic P because PRE (often > 80%) was much higher than rP_i (max < 40%). In principle, the correlations between P resorption and leaf P fractions are determined by the balance between the unit-cost of resorption-derived P and the unit-cost of soil P (Wright and Westoby 2003); that is, preference would be given to obtaining P from the cheapest sources (i.e. P_i). Indeed, PRE was positively correlated with rP_i under relatively P-rich conditions, such as freshwater marshes in northeast China (Mao et al. 2015). We surmise that plants on low-P soils may expend more energy hydrolysing organic P (Hidaka and Kitayama 2011; Tsujii et al. 2017).

Conclusions

The present study is, so far, the most comprehensive survey of leaf P fractions and the LES across wild woody species co-occurring on P-impoverished soils. While the concentration of each P fraction was associated with P-use strategies and N_2-fixation capacity, the relative P fractions were largely independent of the LES, at least among the present set of species, most of which tended towards the 'slow-return' end of the LES. The Proteaceae species in our study, for example, all exhibited low allocations of P to structural constituents (such as cell membrane lipids) and nucleic acids. Presumably, these strategies allow increased P allocation to photosynthesis which, in turn, contributes to high PPUE, regardless of LMA or LL.

Author contribution statement

This study was originated from the research plan designed by YT and IW. YT and BF led the fieldwork with assistance of ZL. YT, and partly ZL, conducted the lab experiments with contributions from BA and HL. YT conducted the data analyses. YT and IW led writing of the manuscript. All authors contributed to the final writing.

Acknowledgements The authors thank Dr Kosala Ranathunge, Dr Roberta Dayrell, and Clément Gille for sharing their protocols of leaf P fractionation and P_i assay. The authors also thank Dr Orpheus Butler for allowing us to use unpublished soil data. Prof Weihua Li helped us for soil total P analysis. Dr Ryota Aoyagi provided valuable comments on an earlier version of the manuscript. Plant material used in this study was collected under NSW National Parks and Wildlife Service Scientific License SL100239.

Funding Open Access funding enabled and organized by CAUL and its Member Institutions YT was supported by JSPS Overseas Research Fellowships and is currently supported by JSPS Postdoctoral fellowships. This work received substantial funding from Macquarie University and JSPS KAKENHI grant to YT (21J00414).

Data availability The datasets generated during and/or analysed during the current study are available from the corresponding author on reasonable request.

Declarations

Competing interests The authors have no relevant financial or non-financial interests.

References

Aerts R (1990) Nutrient use efficiency in evergreen and deciduous species from heathlands. Oecologia 84:391–397. https://doi.org/10.1007/BF00329765

Aoyagi R, Kitayama K (2016) Nutrient allocation among plant organs across 13 tree species in three Bornean rain forests with contrasting nutrient availabilities. J Plant Res 129:675–684. https://doi.org/10.1007/s10265-016-0826-z

Beadle NCW (1954) Soil phosphate and the delimitation of plant communities in eastern Australia. Ecology 35:370–375. https://doi.org/10.2307/1930100

Bernacchi CJ, Singsaas EL, Pimentel C et al (2001) Improved temperature response functions for models of Rubisco-limited photosynthesis. Glob Change Biol 21:253–259. https://doi.org/10.1111/J.1365-3040.2001.00668.X

Bureau of Meteorology, Australian Government. http://www.bom.gov.au/climate/data/. Accessed 19 March 2023

Chabot BF, Hicks DJ (1982) The ecology of leaf life spans. Annu Rev Ecol Syst 13:229–259. https://doi.org/10.1146/annurev.es.13.110182.001305

Chapin FS, Kedrowski RA (1983) Seasonal changes in nitrogen and phosphorus fractions and autumn retranslocation

in evergreen and deciduous taiga trees. Ecology 64:376–391. https://doi.org/10.2307/1937083

Crous KY, Ellsworth DS (2020) Probing the inner sanctum of leaf phosphorus: measuring the fractions of leaf P. Plant Soil 454:77–85. https://doi.org/10.1007/s11104-020-04657-3

Crous KY, Quentin AG, Lin YS et al (2013) Photosynthesis of temperate *Eucalyptus globulus* trees outside their native range has limited adjustment to elevated CO2 and climate warming. Glob Change Biol 19:3790–3807. https://doi.org/10.1111/gcb.12314

Dayrell RLC, Cawthray GR, Lambers H, Ranathunge K (2022) Using activated charcoal to remove substances interfering with the colorimetric assay of inorganic phosphate in plant extracts Abstract. Plant Soil 476:755–764. https://doi.org/10.1007/s11104-021-05195-2

De Kauwe MG, Lin YS, Wright IJ et al (2016) A test of the "one-point method" for estimating maximum carboxylation capacity from field-measured, light-saturated photosynthesis. New Phytol 210:1130–1144. https://doi.org/10.1111/nph.13815

Denton MD, Veneklaas EJ, Freimoser FM, Lambers H (2007) *Banksia* species (Proteaceae) from severely phosphorus-impoverished soils exhibit extreme efficiency in the use and re-mobilization of phosphorus. Plant, Cell Environ 30:1557–1565. https://doi.org/10.1111/j.1365-3040.2007.01733.x

Du E, Terrer C, Pellegrini AFA et al (2020) Global patterns of terrestrial nitrogen and phosphorus limitation. Nat Geosci 13:221–226. https://doi.org/10.1038/s41561-019-0530-4

Ellsworth DS, Crous KY, Lambers H, Cooke J (2015) Phosphorus recycling in photorespiration maintains high photosynthetic capacity in woody species. Plant Cell Environ 38:1142–1156. https://doi.org/10.1111/pce.12468

Elser JJ, Bracken MES, Cleland EE et al (2007) Global analysis of nitrogen and phosphorus limitation of primary producers in freshwater, marine and terrestrial ecosystems. Ecol Lett 10:1135–1142. https://doi.org/10.1111/j.1461-0248.2007.01113.x

Elser JJ, Fagan WF, Kerkhoff AJ et al (2010) Biological stoichiometry of plant production: metabolism, scaling and ecological response to global change. New Phytol 186:593–608. https://doi.org/10.1111/j.1469-8137.2010.03214.x

Escudero A, del Arco JM, Sanz IC, Ayala J (1992) Effects of leaf longevity and retranslocation efficiency on the retention time of nutrients in the leaf biomass of different woody species. Oecologia 90:80–87. https://doi.org/10.1007/BF00317812

Evans JR, Clarke VC (2019) The nitrogen cost of photosynthesis. J Exp Bot 70:7–15. https://doi.org/10.1093/jxb/ery366

Feng YL, Lei YB, Wang RF et al (2009) Evolutionary tradeoffs for nitrogen allocation to photosynthesis versus cell walls in an invasive plant. Proc Natl Acad Sci U S A 106:1853–1856. https://doi.org/10.1073/pnas.0808434106

Guan LL, Wen DZ (2011) More nitrogen partition in structural proteins and decreased photosynthetic nitrogen-use efficiency of *Pinus massoniana* under in situ polluted stress. J Plant Res 124:663–673. https://doi.org/10.1007/s10265-011-0405-2

Guilherme Pereira C, Clode PL, Oliveira RS, Lambers H (2018) Eudicots from severely phosphorus-impoverished environments preferentially allocate phosphorus to their mesophyll. New Phytol 218:959–973. https://doi.org/10.1111/nph.15043

Guilherme Pereira C, Hayes PE, O'Sullivan OS et al (2019) Trait convergence in photosynthetic nutrient-use efficiency along a 2-million year dune chronosequence in a global biodiversity hotspot. J Ecol 107:2006–2023. https://doi.org/10.1111/1365-2745.13158

Han Z, Shi J, Pang J et al (2021) Foliar nutrient allocation patterns in *Banksia attenuata* and *Banksia sessilis* differing in growth rate and adaptation to low-phosphorus habitats. Ann Bot 128:419–430. https://doi.org/10.1093/aob/mcab013

Hawkesford MJ, Cakmak I, Coskun D, De Kok LJ, Lambers H, Schjoerring JK, White PJ (2023) Chapter 6: Functions of Macronutrients. In: Rengel Z, Cakmak I, White PJ (eds) Marschner's mineral nutrition of plants, fourth. Academic Press Inc. (London) Ltd., London, pp 201–281

Hayes P, Turner BL, Lambers H, Laliberté E (2014) Foliar nutrient concentrations and resorption efficiency in plants of contrasting nutrient-acquisition strategies along a 2-million-year dune chronosequence. J Ecol 102:396–410. https://doi.org/10.1111/1365-2745.12196

Hayes PE, Adem GD, Pariasca-Tanaka J, Wissuwa M (2022) Leaf phosphorus fractionation in rice to understand internal phosphorus-use efficiency. Ann Bot 129:287–302. https://doi.org/10.1093/aob/mcab138

Hayes PE, Clode PL, Oliveira RS, Lambers H (2018) Proteaceae from phosphorus-impoverished habitats preferentially allocate phosphorus to photosynthetic cells: An adaptation improving phosphorus-use efficiency. Plant Cell Environ 41:605–619. https://doi.org/10.1111/pce.13124

He X, Augusto L, Goll DS et al (2021) Global patterns and drivers of soil total phosphorus concentration. Earth Syst Sci Data 13:5831–5846. https://doi.org/10.5194/essd-13-5831-2021

Hidaka A, Kitayama K (2013) Relationship between photosynthetic phosphorus-use efficiency and foliar phosphorus fractions in tropical tree species. Ecol Evol 3:4872–4880. https://doi.org/10.1002/ece3.861

Hidaka A, Kitayama K (2011) Allocation of foliar phosphorus fractions and leaf traits of tropical tree species in response to decreased soil phosphorus availability on Mount Kinabalu, Borneo. J Ecol 99:849–857. https://doi.org/10.1111/j.1365-2745.2011.01805.x

Jeffrey DW (1964) The formation of polyphosphate in *Banksia Ornata*, an Australian heath plant. Aust J Biol Sci 17:845–854. https://doi.org/10.1071/BI9640845

Kazakou E, Garnier E, Gimenez O (2007) Contribution of leaf life span and nutrient resorption to mean residence time: Elasticity analysis. Ecology 88:1857–1863. https://doi.org/10.1890/06-1352.1

Kedrowski RA (1983) Extraction and analysis of nitrogen, phosphorus and carbon fractions in plant material. J Plant Nutr 6:989–1011. https://doi.org/10.1080/01904168309363161

Killingbeck KT (1996) Nutrients in senesced leaves: Keys to the search for potential resorption and resorption proficiency. Ecology 77:1716–1727. https://doi.org/10.2307/2265777

Kitayama K, Aiba S (2002) Ecosystem structure and productivity of tropical rain forests along altitudinal gradients with contrasting soil phosphorus pools on Mount Kinabalu, Borneo. J Ecol 90:37–51. https://doi.org/10.1046/j.0022-0477.2001.00634.x

Kooyman RM, Laffan SW, Westoby M (2017) The incidence of low phosphorus soils in Australia. Plant Soil 412:143–150. https://doi.org/10.1007/s11104-016-3057-0

Kumar A, Singh B, Raigond P et al (2021) Phytic acid: Blessing in disguise, a prime compound required for both plant and human nutrition. Food Res Int 142:110193. https://doi.org/10.1016/j.foodres.2021.110193

Lambers H (2022) Phosphorus Acquisition and Utilization in Plants. Annu Rev Plant Biol 73:17–42. https://doi.org/10.1146/annurev-arplant-102720-125738

Lambers H, Cawthray GR, Giavalisco P et al (2012) Proteaceae from severely phosphorus-impoverished soils extensively replace phospholipids with galactolipids and sulfolipids during leaf development to achieve a high photosynthetic phosphorus-use-efficiency. New Phytol 196:1098–1108. https://doi.org/10.1111/j.1469-8137.2012.04285.x

Lambers H, Oliveira RS (2019) Plant Physiological Ecology, Third edit. Springer International Publishing, Cham

Lambers H, Poorter H (2004) Inherent variation in growth rate between higher plants: a search for physiological causes and ecological consequences. Adv Ecol Res 34:283–362. https://doi.org/10.1016/S0065-2504(03)34004-8

Lawrie AC (1982) Field nodulation in nine species of *Casuarina* in Victoria. Aust J Bot 30:447–460. https://doi.org/10.1071/BT9820447

Lei Y, Du L, Chen K et al (2021) Optimizing foliar allocation of limiting nutrients and fast-slow economic strategies drive forest succession along a glacier retreating chronosequence in the eastern Tibetan Plateau. Plant Soil 462:159–174. https://doi.org/10.1007/s11104-020-04827-3

Mao R, Zeng D-H, Zhang X-H, Song C-C (2015) Responses of plant nutrient resorption to phosphorus addition in freshwater marsh of Northeast China. Sci Rep 5:8097. https://doi.org/10.1038/srep08097

Miyachi S, Tamiya H (1961) Distribution and turnover of phosphate compounds in growing *Chlorella* cells. Plant Cell Physiol 414:405–414. https://doi.org/10.1093/oxfordjournals.pcp.a077695

Mo Q, Li Z, Sayer EJ et al (2019) Foliar phosphorus fractions reveal how tropical plants maintain photosynthetic rates despite low soil phosphorus availability. Funct Ecol 33:503–513. https://doi.org/10.1111/1365-2435.13252

Murphy J, Riley JP (1962) A modified single solution method for the determination of phosphate in natural waters. Anal Chim Acta 27:31–36. https://doi.org/10.1016/S0003-2670(00)88444-5

Olsen S, Sommers L (1982) No Title. In: Page A, Miller R, Keeney D (eds) Methods of Soil Analysis, Agronomy Series No.9, Part 2., 2nd edn. Madison, WI, USA: Soil Science Society ofAmerica, pp 403–430

Onoda Y, Hikosaka K, Hirose T (2004) Allocation of nitrogen to cell walls decreases photosynthetic nitrogen-use efficiency. Funct Ecol 18:419–425. https://doi.org/10.1111/j.0269-8463.2004.00847.x

Onoda Y, Wright IJ, Evans JR et al (2017) Physiological and structural tradeoffs underlying the leaf economics spectrum. New Phytol 214:1447–1463. https://doi.org/10.1111/nph.14496

R Core Team (2020) R: A language and environment for statistical computing. R Found Stat Comput Vienna, Austria URL https//wwwR-project.org/

Reich PB, Oleksyn J, Wright IJ et al (2010) Evidence of a general 2/3-power law of scaling leaf nitrogen to phosphorus among major plant groups and biomes. Proc R Soc B Biol Sci 277:877–883. https://doi.org/10.1098/rspb.2009.1818

Reich PB, Walters MB, Ellsworth DS (1997) From tropics to tundra: Global convergence in plant functioning. Proc Natl Acad Sci U S A 94:13730–13734. https://doi.org/10.1073/pnas.94.25.13730

Rodríguez-Echeverría S, Crisóstomo JA, Nabais C, Freitas H (2009) Belowground mutualists and the invasive ability of Acacia longifolia in coastal dunes of Portugal. Biol Invasions 11:651–661. https://doi.org/10.1007/s10530-008-9280-8

Shane MW, Lambers H (2005) Cluster roots: A curiosity in context. Plant Soil 274:101–125. https://doi.org/10.1007/s11104-004-2725-7

Shane MW, McCully ME, Lambers H (2004) Tissue and cellular phosphorus storage during development of phosphorus toxicity in *Hakea prostrata* (Proteaceae). J Exp Bot 55:1033–1044. https://doi.org/10.1093/jxb/erh111

Shipley B, Lechowicz MJ, Wright I, Reich PB (2006) Fundamental trade-offs generating the worldwide leaf economics spectrum. Ecology 87:535–541. https://doi.org/10.1890/05-1051

Suriyagoda LDB, Ryan MH, Gille CE et al (2023) Phosphorus fractions in leaves. New Phytol 237:1122–1135. https://doi.org/10.1111/nph.18588

Takahashi T, Hikosaka K, Hirose T (2004) Photosynthesis or persistence: nitrogen allocation in leaves of evergreen and deciduous Quercus species. Plant, Cell Environ 27:1047–1054. https://doi.org/10.1111/j.1365-3040.2004.01209.x

Thornley JHM, Cannell MGR (2000) Modelling the components of plant respiration: Representation and realism. Ann Bot 85:55–67. https://doi.org/10.1006/anbo.1999.0997

Tian D, Yan Z, Niklas KJ et al (2018) Global leaf nitrogen and phosphorus stoichiometry and their scaling exponent. Natl Sci Rev 5:728–739. https://doi.org/10.1093/nsr/nwx142

Tiessen H, Moir J (1993) Characterization of available P by sequential extraction. In: Carter MR (ed) Soil sampling and methods of analysis. First Lewis Publishers, Boca Raton, pp 75–86

Tsujii Y, Aiba S, Kitayama K (2020) Phosphorus allocation to and resorption from leaves regulate the residence time of phosphorus in above-ground forest biomass on Mount Kinabalu, Borneo. Funct Ecol 34:1702–1712. https://doi.org/10.1111/1365-2435.13574

Tsujii Y, Onoda Y, Kitayama K (2017) Phosphorus and nitrogen resorption from different chemical fractions in senescing leaves of tropical tree species on Mount Kinabalu, Borneo. Oecologia 185:171–180. https://doi.org/10.1007/s00442-017-3938-9

Veneklaas EJ, Lambers H, Bragg J et al (2012) Opportunities for improving phosphorus-use efficiency in crop plants. New Phytol 195:306–320. https://doi.org/10.1111/j.1469-8137.2012.04190.x

Vergutz L, Manzoni S, Porporato A et al (2012) Global resorption efficiencies and concentrations of carbon and nutrients in leaves of terrestrial plants. Ecol Monogr 82:205–220. https://doi.org/10.1890/11-0416.1

Vitousek PM, Porder S, Houlton BZ, Chadwick OA (2010) Terrestrial phosphorus limitation: mechanisms,

implications, and nitrogen–phosphorus interactions. Ecol Appl 20:5–15. https://doi.org/10.1890/08-0127.1

Westerband AC, Wright IJ, Maire V et al (2022) Coordination of photosynthetic traits across soil and climate gradients. Glob Change Biol 856–873. https://doi.org/10.1111/gcb.16501

Westoby M, Falster DS, Moles AT et al (2002) Plant ecological strategies: Some leading dimensions of variation between species. Annu Rev Ecol Syst 33:125–159. https://doi.org/10.1146/annurev.ecolsys.33.010802.150452

White PJ, Hammond JP (2008) Phosphorus nutrition of terrestrial plants. In: White PJ, Hammond JP (eds) The Ecophysiology of Plant-Phosphorus Interactions. Springer, Dordrecht, pp 51–81

Wickham H (2016) ggplot2: Elegant Graphics for Data Analysis. Springer-Verlag, New York

Willemot C (1975) Stimulation of phospholipid biosynthesis during frost hardening of winter wheat. Plant Physiol 55:356–359. https://doi.org/10.1104/pp.55.2.356

Wright IJ, Reich PB, Cornelissen JHC et al (2005) Assessing the generality of global leaf trait relationships. New Phytol 166:485–496. https://doi.org/10.1111/j.1469-8137.2005.01349.x

Wright IJ, Reich PB, Westoby M (2001) Strategy-shifts in leaf physiology, structure and nutrient content between species of high and low rainfall, and high and low nutrient habitats. Funct Ecol 15:423–434. https://doi.org/10.1046/j.0269-8463.2001.00542.x

Wright IJ, Reich PB, Westoby M et al (2004) The worldwide leaf economics spectrum. Nature 428:821–827. https://doi.org/10.1038/nature02403

Wright IJ, Westoby M (2003) Nutrient concentration, resorption and lifespan: Leaf traits of Australian sclerophyll species. Funct Ecol 17:10–19. https://doi.org/10.1046/j.1365-2435.2003.00694.x

Wright IJ, Westoby M (2002) Leaves at low versus high rainfall: coordination of structure, lifespan and physiology. New Phytol 155:403–416. https://doi.org/10.1046/j.1469-8137.2002.00479.x

Wright IJ, Westoby M, Reich PB (2002) Convergence towards higher leaf mass per area in dry and nutrient-poor habitats has different consequences for leaf life span. J Ecol 90:534–543. https://doi.org/10.1046/j.1365-2745.2002.00689.x

Yan L, Sunoj VSJ, Short AW et al (2021) Correlations between allocation to foliar phosphorus fractions and maintenance of photosynthetic integrity in six mangrove populations as affected by chilling. New Phytol 232:2267–2282. https://doi.org/10.1111/nph.17770

Yan L, Zhang X, Han Z et al (2019) Responses of foliar phosphorus fractions to soil age are diverse along a 2 Myr dune chronosequence. New Phytol 223:1621–1633. https://doi.org/10.1111/nph.15910

Yoshida S, Sakai A (1973) Phospholipid changes associated with the cold hardiness of cortical cells from poplar stem. Plant Cell Physiol 14:353–359. https://doi.org/10.1093/oxfordjournals.pcp.a074867